Journal of Electron Spectroscopy and Related Phenomena 279 (2025) 147514

Contents lists available at ScienceDirect

Journal of Electron Spectroscopy and Related Phenomena

journal homepage: www.elsevier.com/locate/elspec

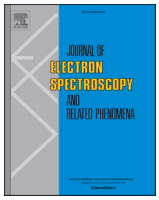

# Anisotropic dispersion of excitonic bands of the single-crystal pentacene (001) surface as measured by low-energy angle-resolved high-resolution electron energy-loss spectroscopy

Yasuo Nakayama [a,b,c,*], François C. Bocquet [d,e], Ryohei Tsuruta [f], Serguei Soubatch [d,e], F. Stefan Tautz [d,e,g]

[a] Department of Pure and Applied Chemistry, Tokyo University of Science (TUS), 2641 Yamazaki, Noda 278-8510, Japan
[b] Division of Colloid and Interface Science, Tokyo University of Science, 2641 Yamazaki, Noda 278-8510, Japan
[c] Research Group for Advanced Energy Conversion, Tokyo University of Science, 2641 Yamazaki, Noda 278-8510, Japan
[d] Peter Grünberg Institut (PGI-3), Forschungszentrum Jülich, Jülich 52425, Germany
[e] Jülich Aachen Research Alliance (JARA) Fundamentals of Future Information Technology, Jülich 52425, Germany
[f] Faculty of Pure and Applied Sciences, University of Tsukuba, 1-1-1 Tennodai, Tsukuba, Ibaraki 305-8577, Japan
[g] Experimentalphysik IV A, RWTH Aachen University, Aachen 52074, Germany

ARTICLE INFO

*Keywords:*
Organic semiconductor
Single crystal
EELS
Exciton
Vibration

ABSTRACT

Low-energy high-resolution electron energy-loss spectroscopy (HREELS) is a useful technique for the characterization of various excitation processes at solid surfaces. However, no successful work has been reported on molecular single-crystal samples yet. In the present study, low-energy angle-resolved HREELS measurements were conducted on single-crystal pentacene, an organic semiconductor. The results confirmed the excitonic bands exhibiting energy–momentum dispersion and anisotropy of these depending on the surface crystallographic directions, corroborating the occurrence of exciton delocalization, contrary to the ordinary notion of the Frenkel exciton for weakly interacting van der Waals molecular solids. The present results demonstrate that low-energy angle-resolved HREELS is applicable to the precise examination of the excitonic characteristics of solid-state surfaces, even for molecular semiconductor single crystals.

## 1. Introduction

The exciton, a quasiparticle representing a pair of an electron and a hole bound to each other due to Coulombic interactions, is typically used to describe photon-electron interconversion in semiconductor optoelectronic devices. In molecular solids, they are commonly considered to be localized within individual molecules, similar to the case of individual electrons and holes. In contrast to this conventional notion, substantial delocalization of the electronic states over several molecules occurs in various crystalline organic semiconductor species. This delocalization is indicated by the observation of energy–momentum dispersion of the electronic bands, which can be measured using angle-resolved photoelectron spectroscopy (AR-PES) [1,2]. The excitonic characteristics in such molecular crystals presumably deviate from those of ordinary single-molecular Frenkel excitons and thus represent a research subject of great interest [3,4].

Electron energy-loss spectroscopy (EELS) is an experimental technique that probes the energy loss due to inelastic scattering of electrons incident onto a sample, allowing the characterization of various excitation processes of solid-state materials [5–8]. With angle-resolved high-resolution EELS (AR-HREELS), the monochromatized electron energy and collimated electron beam enable the measurement of the energy–momentum dispersion relations of quasiparticles in solids, since the distributions of the energy and direction of scattered electrons are independently analyzed [9–11]. Practical realizations of EELS can be categorized based on the energy of the primary electron beam into high-energy (a few hundred keV) and low-energy (several hundred eV or lower) techniques: in the former case, the electrons scattered and transmitted through the sample are analyzed, while the latter technique deals with the electrons reflected from the sample surface [6]. Whereas the high-energy EELS has been successfully applied to molecular semiconductor single-crystal samples [12–15], one restriction in measurable

* Corresponding author at: Department of Pure and Applied Chemistry, Tokyo University of Science (TUS), 2641 Yamazaki, Noda 278-8510, Japan.
*E-mail address:* nkym@rs.tus.ac.jp (Y. Nakayama).

https://doi.org/10.1016/j.elspec.2025.147514
Received 9 September 2024; Received in revised form 8 January 2025; Accepted 13 January 2025
Available online 31 January 2025

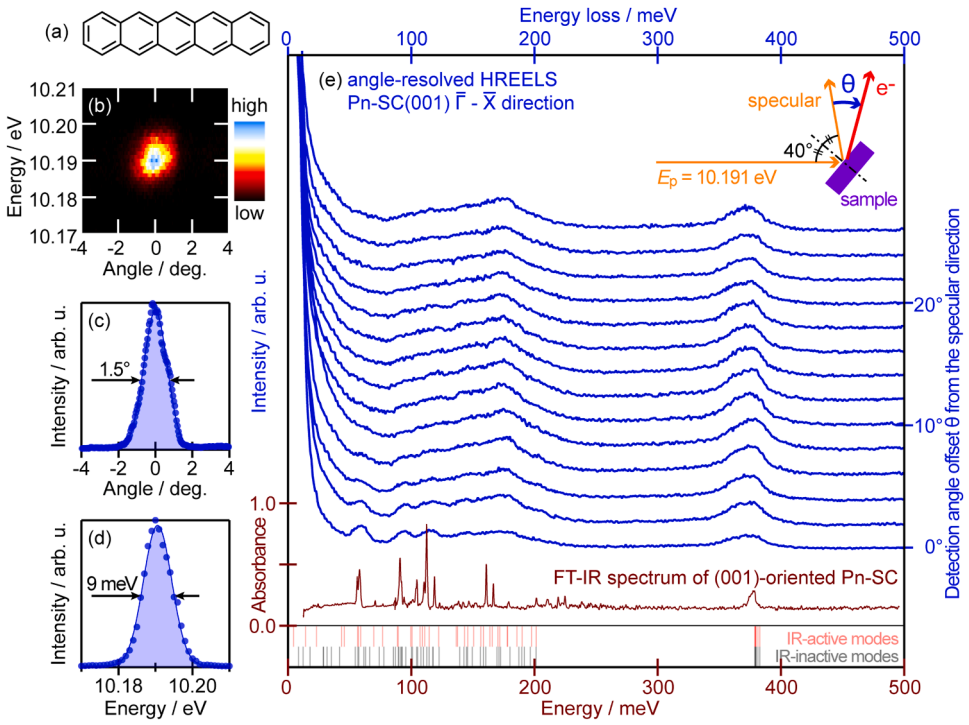


**Fig. 1.** (a) Molecular structure of pentacene. (b) Typical electron beam spot for the specular reflection from the Pn-SC(001) sample. (c) Profile of (b) in the angular direction. (d) Profile of (b) in the energy direction. (e) AR-HREELS spectra in the energy range corresponding to the vibronic energy losses for the Pn-SC(001) surface measured in the $\bar{\Gamma}-\bar{X}$ direction. For clarity, the spectra with different electron detection angles θ are vertically offset from the spectrum for the specular direction. The red curve represents the FT-IR absorbance spectrum through a (001)-oriented Pn-SC sample taken from Ref. [48]. Results of a quantum chemical calculation for the frequencies of IR-active and IR-inactive vibration modes for a single pentacene molecule are displayed as pale-red and gray vertical bars, respectively. (Inset) Schematic drawing of the measurement geometry.

systems is that the sample has to be microtomed to allow transmission of the electron beam. In contrast, low-energy EELS is applicable to specimens without such pretreatments and is generally used as a surface analysis technique because of the short mean-free-path of the electrons (with energies ranging from a few ten to a few hundred eV) inside solids [16,17]. Despite several studies applying this methodology to organic semiconductor materials [18–25], no successful results on molecular semiconductor single-crystal samples have been reported so far.

In this study, low-energy AR-HREELS measurements were conducted on the single-crystal surface of pentacene ($C_{22}H_{14}$, Fig. 1(a)). This molecule is one of the most intensively studied organic semiconductors and is known to exhibit energy–momentum dispersion of its electronic bands [26–35], thereby displaying high charge carrier mobility [36–38] in its crystalline phases. In addition, pentacene is well-known for its high singlet fission efficiency [39–43], which has attracted particular interest regarding the excitonic characteristics of this material. Our experiments successfully confirmed the energy–momentum dispersion of the lowest singlet excitonic state as well as its anisotropy depending on the surface crystallographic directions. The present results demonstrate that low-energy AR-HREELS is applicable to molecular single-crystal surfaces for the elucidation of their various excitation processes.

## 2. Experimental

Pentacene single-crystal (Pn-SC) samples were produced by a horizontal physical vapor transport technique in a purified nitrogen ($N_2$) stream with an apparatus described in Ref. [44]. The obtained plate-shaped crystal pieces of pentacene are generally single-crystalline with a (001) surface, however, misoriented crystal fragments often adhere on the surface as detected previously [45]. The crystals were directly transferred into a $N_2$-filled glovebox. They were glued onto Au-coated Si wafer pieces with conductive Ag paste to ensure sufficient electrical contact [2], and then encapsulated within an airtight container. To minimize the exposure of the Pn-SC samples to the ambient atmosphere and thus to avoid the formation of oxidized species on the surface [46], the samples were introduced into the HREELS equipment by using a plastic bag (glove bag) filled with $N_2$ [34].

AR-HREELS experiments were carried out using a measurement system reported previously [11]. Primary electrons monochromatized by two 146°-deflectors were focused at the sample position by a specially designed electron transfer lens system. Electrons scattered at the sample surface were detected by a hemispherical electron analyzer (Scienta R4000) in a two-dimensional (2D) manner: one axis of the recorded intensity distribution corresponds to the scattering angle along a certain crystallographic orientation of the sample, while the other axis corresponds to the electron kinetic energy. The primary electron energy $E_p$ was accurately determined by the specular electron profiles. The specular reflection spot as typically observed on the 2D electron detector is shown in Fig. 1(b). The crystallographic orientation of the Pn-SC sample was specified using low-energy electron diffraction enhanced by a micro-channel plate detector (MCP-LEED) and then was accurately determined by detection of the 100 and 010 Bragg spots. To enhance photoconductivity and thus prevent charging of the sample [47], the sample was illuminated by continuous-wave laser light with a wavelength of 445 nm for the MCP-LEED and of 405 nm for the HREELS measurements. All measurements were conducted at room temperature (RT).

## 3. Results and discussion

First, the electron energy-loss features in an energy range lower than the electronic excitation are briefly described. Fig. 1(e) shows AR-HREELS spectra in an energy-loss range of 0 – 0.5 eV for the Pn-SC (001) surface, measured along its **a***-axis ($\bar{\Gamma}-\bar{X}$ direction). For

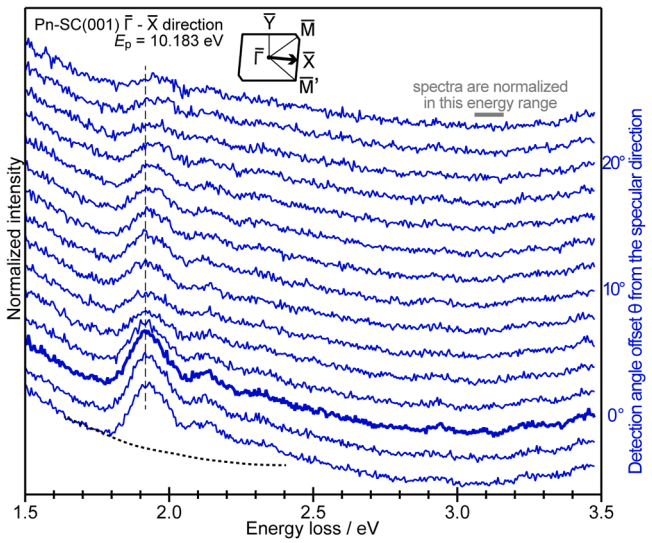


**Fig. 2.** AR-HREELS spectra in the energy range corresponding to the excitonic energy-losses at the Pn-SC(001) surface measured in the $\overline{\Gamma}-\overline{X}$ direction. The spectra are normalized by the intensity measured in the energy range of 3.1 – 3.2 eV, where no prominent structure was observed at any angle, and are vertically offset for different θ for clarity. The spectrum corresponding to the specular direction (θ = 0°) is highlighted with a thick line, and the energy position of its smallest energy-loss peak is indicated with a vertical dashed line. A background curve deduced from the slope at the smaller energy-loss side of the first excitonic peak is displayed as a dotted line. (Inset) Surface Brillouin zone of the Pn-SC(001) surface.

comparison, a Fourier transform infrared (FT-IR) absorption spectrum of Pn-SC measured in transmission geometry along its **c***-axis is represented together with quantum chemical calculation results for the energy distribution of the intramolecular vibrational modes [48]. Peaks observed in the energy range of 0.35 – 0.4 eV are attributed to C–H stretching modes, while spectral features below 0.2 eV originate from energy transfer to lower-frequency vibrational modes such as C–C stretching modes, C–H and C–C bending modes, and so on. For small values of θ (electron detection angle close to the specular reflection), several energy-loss components are resolved in the low-energy region, whose energies correspond well to the FT-IR peaks as well as the calculated vibrational frequencies. Further increase in the detection angle offset from the specular direction resulted in a broadening of these spectral components. A detailed discussion on the characteristics of individual vibrational modes is difficult because the present measurements lack sufficient energy resolution. Nevertheless, it can be clearly seen that within this energy loss range corresponding to the molecular vibronic excitations, no energy shift of the spectral components was observed.

We now turn to AR-HREELS spectra in the excitonic energy-loss region along the $\overline{\Gamma}-\overline{X}$ direction of the Pn-SC(001) surface, shown in Fig. 2. In the energy range of 1.8 – 2.5 eV, the spectral components reproduce characteristics of spectroscopic ellipsometry results on single-crystal pentacene [49] fairly well. The peak intensities are strongly reduced upon increasing the detection angle away from the specular angle, as also observed in the vibrational energy region. Nevertheless, two spectral peaks in the energy range 1.8 – 2.2 eV are resolved across the whole θ range. In contrast to the case of the vibrational energy region, Fig. 2 clearly shows that the first peak exhibits an obvious energy shift to higher energy-loss values when increasing θ relative to the specular reflection angle.

Further analysis of the excitonic states needs adequate removal of the background (BG) intensity from the spectra, which was performed for the present case in the following two steps: (1) a baseline function proportional to $E_k^{1.5}$ (where $E_k$ is the kinetic energy) was assumed by the extrapolation of the intensity slope in an $E_k$ range higher than the onset of the first excitonic peak ($E_k$ = 8.43 – 8.55 eV), and (2) an additional BG intensity at each energy position assumed to be proportional to the integrated intensity of the baseline-subtracted spectra from the excitonic peak onset to the respective energy was further removed. A BG intensity profile for one HREELS spectrum is exemplified in Fig. 2 by the dotted curve. The energy shift of the excitonic energy-loss peaks can be recognized more distinctly for the BG-subtracted spectra as mapped in Fig. 3 as a function of the momentum transfer **q** in the in-plane directions. In the $\overline{\Gamma}-\overline{X}$ direction, it is clearly seen that the first peak, located at an approximate energy loss value of 1.9 eV ($E_k \sim 8.3$ eV) for the specular direction ($\overline{\Gamma}$ point), shifts to the lower $E_k$ side upon increasing **q** toward the $\overline{X}$ point, as shown in Fig. 3(a). Fig. 3(b), (c), and (d) are the BG-subtracted AR-HREELS spectra measured in the $\overline{\Gamma}-\overline{Y}$, $\overline{\Gamma}-\overline{M}$, and $\overline{\Gamma}-\overline{M'}$ directions, respectively. In the $\overline{\Gamma}-\overline{Y}$ direction, the smallest energy-loss component exhibits a significant intensity drop as predicted theoretically [50,51], and thus, the first peak exhibits the maximal intensity in the middle of the Brillouin zone (BZ). On the other hand, the overall trends in the shifts for the $\overline{\Gamma}-\overline{M}$ and $\overline{\Gamma}-\overline{M'}$ directions are considered to be similar to that of the $\overline{\Gamma}-\overline{X}$ direction.

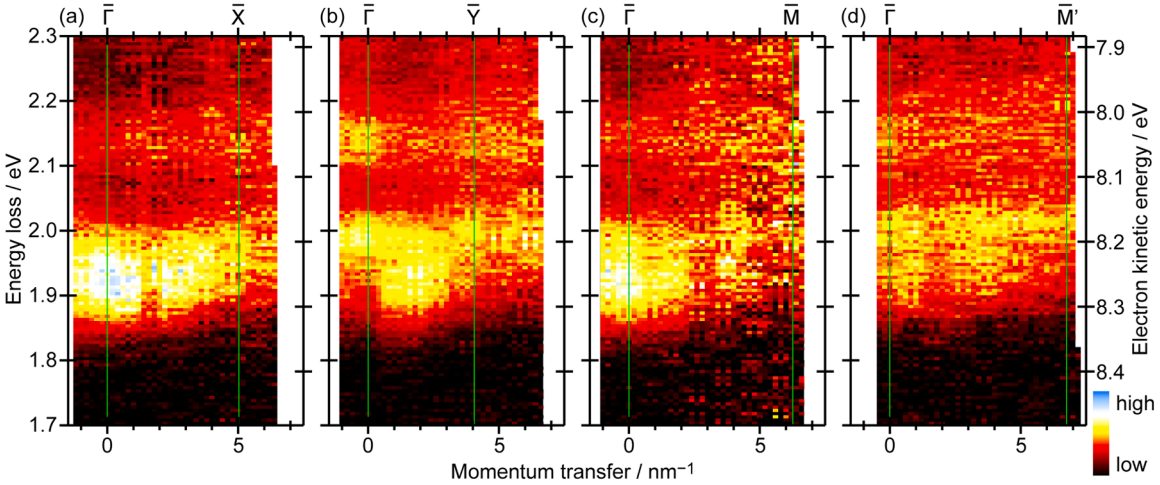


**Fig. 3.** 2D mapping image of AR-HREELS spectra of Pn-SC(001), taken in the (a) $\overline{\Gamma}-\overline{X}$, (b) $\overline{\Gamma}-\overline{Y}$, (c) $\overline{\Gamma}-\overline{M}$, and (d) $\overline{\Gamma}-\overline{M'}$ directions. The background intensity was subtracted from the raw spectra, and the displayed intensity was normalized by the total intensity for each angle. The right axis indicates the electron kinetic energy for each spectrum, and the left axis is based on the common energy-loss range for all four images.

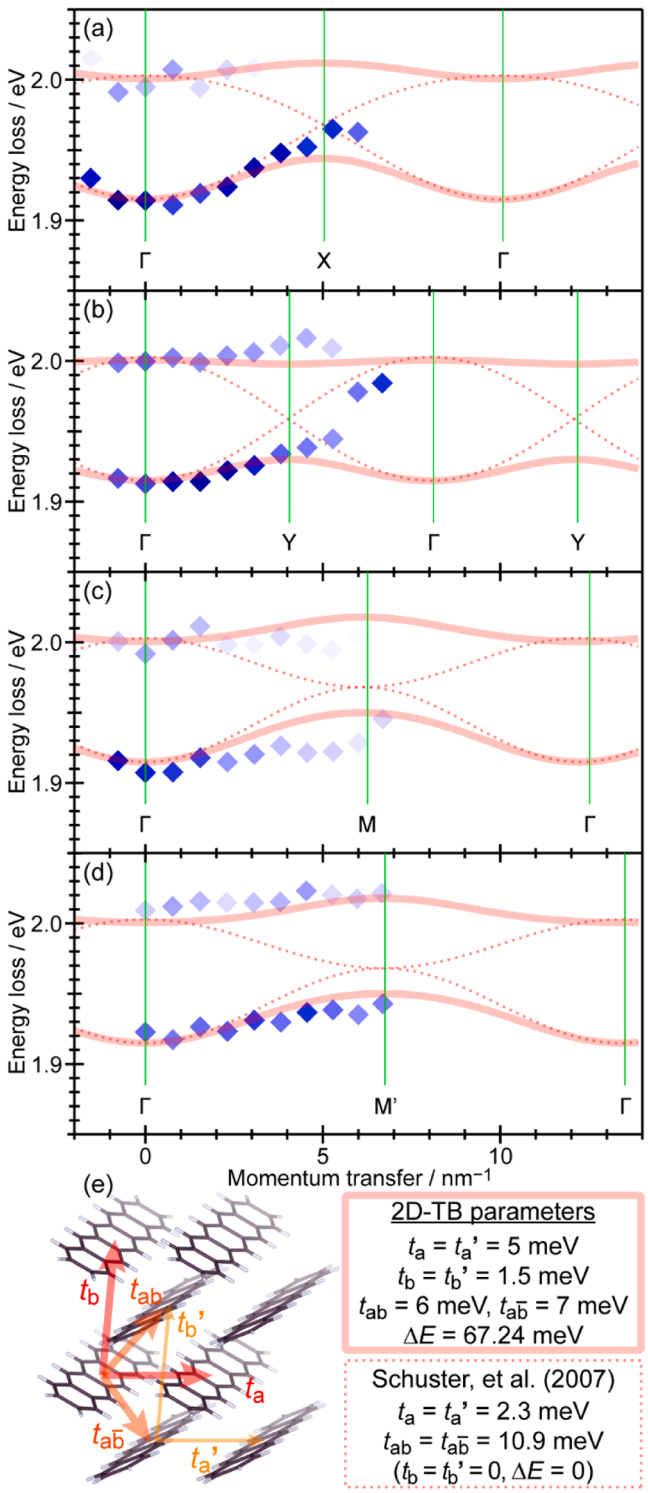


**Fig. 4.** (a – d) Excitonic energy-loss peak positions plotted as a function of in-plane momentum transfer for the (a) $\overline{\Gamma} - \overline{X}$, (b) $\overline{\Gamma} - \overline{Y}$, (c) $\overline{\Gamma} - \overline{M}$, and (d) $\overline{\Gamma} - \overline{M}'$ directions. The color tone of the symbol represents the peak intensity (dark: intense, pale: weak). The thick solid curves display the best fit results for the energy-momentum relations in the two-dimensional TB formulation [27], whereas the thin dotted curves correspond to those using the parameters suggested in Ref. [54]. (e) Schematic illustration of the molecular arrangement of the (001) surface of single-crystal pentacene and transfer integrals to the adjacent molecules taken into account for the present TB analysis.

The energies of excitonic losses are determined by least-squares fitting of the individual BG-subtracted HREELS spectra. These positions are plotted as a function of **q** in the in-plane directions for the $\overline{\Gamma} - \overline{X}$, $\overline{\Gamma} - \overline{Y}$, $\overline{\Gamma} - \overline{M}$, and $\overline{\Gamma} - \overline{M}'$ directions in Fig. 4(a), (b), (c), and (d), respectively. Around the $\overline{\Gamma}$ point, the 1st excitonic peak of each spectrum is further separated into two components separated from each other by 85 ± 4 meV. This could be attributed to the Davydov splitting. However, the present energy split was narrower than the past theoretical and experimental values (0.12 – 0.15 eV [14,15,50–52]), and the energy position of the greater energy-loss component is substantially independent of the momentum, contradicting the theoretical prediction [52]. Another possible explanation for this energy splitting is symmetric and antisymmetric exchange interactions of the electron-hole pairs between two inequivalent pentacene molecules, as predicted by another theoretical work [51]. A clear conclusion about this point cannot be deduced from the present results. Nevertheless, the smaller energy-loss component shifts to a higher energy-loss value by approximately 0.05 eV when moving from $\overline{\Gamma}$ to $\overline{X}$. On the other hand, the energy of the second excitonic peak at 2.1 – 2.2 eV does not change with θ. Similar behaviors are also observed in the $\overline{\Gamma} - \overline{Y}$, $\overline{\Gamma} - \overline{M}$, and $\overline{\Gamma} - \overline{M}'$ directions.

Knupfer, Berger, and coworkers reported the energy dispersion of the lowest singlet excitonic state of Pn-SC(001) measured by high-energy ($E_p$ = 170 keV) HREELS in wide $|\mathbf{q}|$ ranges up to 16 nm$^{-1}$ except for around the reciprocal space origin ($|\mathbf{q}| < 0.8$ nm$^{-1}$). These results were concluded to represent significant evidence for the generation of "charge-transfer (CT) excitons" released from single-molecule confinement [12,14,15,53,54]. They also demonstrated the azimuthal orientation-dependent anisotropy of the excitonic energy dispersion: in the $\overline{\Gamma} - \overline{X}$ and $\overline{\Gamma} - \overline{M}$ directions, leading edge energies of the excitonic energy-loss peaks reached a minimum near the reciprocal space origin and increased when approaching each next reciprocal point. These energy-momentum dispersion trends $E_{\pm}(\mathbf{q})$ of two Davydov branches of the excitonic bands are modeled by a tight-binding (TB) description in the two-dimensional manner as in Ref. [27]:

$$E_{\pm}(\mathbf{q}) = E_0 - 2(t_a\cos[\mathbf{q}\cdot\mathbf{a}] + t_b\cos[\mathbf{q}\cdot\mathbf{b}]) \pm \sqrt{\left(\frac{\Delta E}{2}\right)^2 + 4\left(t_{ab}\cos\left[\mathbf{q}\cdot\left(\frac{\mathbf{a}+\mathbf{b}}{2}\right)\right] + t_{a\bar{b}}\cos\left[\mathbf{q}\cdot\left(\frac{\mathbf{a}-\mathbf{b}}{2}\right)\right]\right)^2},$$

where $t$ are the transfer integrals, $\Delta E$ is the energy difference between the two inequivalent sites, and $E_0$ is the excitonic energy of the isolated molecules.

Intermolecular transfer integrals are assumed to be negligibly small except for those of the molecular combinations indicated in Fig. 4(e), and the interactions between translationally equivalent molecules are set equal for two inequivalent pentacene molecules in the unit cell (i.e., $t_a' = t_a$ and $t_b' = t_b$). Using previously reported lattice constants of single-crystal pentacene [55], this TB modeling reproduces the present results as displayed in Fig. 4(a – d), where the transfer integrals $t_a$, $t_b$, $t_{ab}$, and $t_{a\bar{b}}$ are assumed to be 5 ± 1 meV, 1.5 ± 0.5 meV, 6 ± 2 meV, and 7 ± 2 meV, respectively. On the other hand, the values ($t_a$ = 2.3 meV and $t_{ab}$ = 10.9 meV) reported in the literature [54] fail to reproduce the present results except for the $\overline{\Gamma} - \overline{X}$ direction as presented as dotted curves in Fig. 4(a – d).[1] For the present best fit TB curves (solid lines), although some mismatch was found for large **q** values which can be ascribed to inaccurate peak positions caused by vanishing peak intensities, the calculated dispersion trends well agree with the experimental

[1] The TB formula given in Ref [54] is derived by putting $\Delta E = 0$ and $t_{a\bar{b}} = t_{ab}$ and by inverting the signs of transfer integrals. The value of $t_b$ was not presented in that literature. In this article, $t_b = 0$, $t_{a\bar{b}} = t_{ab}$, and $\Delta E = 0$ are assumed to reproduce the $E(\mathbf{q})$ relations based on the literature parameters.

energy-momentum relations. This confirms the presence of the delocalized CT characters of the excitons and an anisotropy of the intermolecular excitonic couplings at the surface of the single-crystal pentacene. Nevertheless, further work is necessary to perform a more precise analysis of the excitonic energy dispersions in wider momentum ranges under optimized conditions where, e.g., greater excitonic energy-loss intensity can be achieved.

## 4. Conclusions

In this study, HREELS measurements with a low electron primary energy of 10 eV were performed on molecular single-crystal samples of an organic semiconductor pentacene. AR-HREELS spectra revealed that the energy shift of the lowest singlet exciton-derived energy-loss peak depends on the electron scattering angle with respect to the specular direction, thereby confirming that the excitons exhibit energy–momentum dispersion. Furthermore, different dispersion trends were observed along different crystal high-symmetry directions by in-plane azimuthal angle dependence. The present results indicate the applicability of low-energy AR-HREELS to demonstrate delocalized CT excitonic states at the surfaces of molecular semiconductor single crystals, just as AR-PES is able to assess charge carrier delocalization. This opens further possibilities for spectroscopic analyses of the excitonic characteristics at well-defined molecular heterojunctions built on molecular single-crystal surfaces [56,57].

## CRediT authorship contribution statement

**F. Stefan Tautz:** Supervision, Resources, Funding acquisition. **Ryohei Tsuruta:** Resources. **Serguei Soubatch:** Conceptualization. **Yasuo Nakayama:** Writing – review & editing, Writing – original draft, Visualization, Project administration, Investigation, Funding acquisition, Formal analysis, Conceptualization. **François C. Bocquet:** Software, Methodology, Funding acquisition.

## Declaration of Competing Interest

The authors declare that they have no known competing financial interests or personal relationships that could have appeared to influence the work reported in this paper.

## Acknowledgments

This work was financially supported by JSPS-KAKENHIs [Grant Nos. JP23K23323 (JP22H02055) and JP21H05405], The Futaba Foundation, and Morino Foundation for Molecular Science. Y.N. would like to thank the Overseas Sabbatical Program of TUS. F.S.T. and F.C.B. acknowledge funding by the DFG through the SFB 1083 Structure and Dynamics of Internal Interfaces (project A12). F.S.T. acknowledges funding by the European Union through the ERC Synergy grant Orbital Cinema (101071259).

## Data availability

All data needed to evaluate the conclusions in the paper are present in the paper. Raw data used to produce the figures are available at the Jülich DATA public repository [58].

## References

[1] Y. Nakayama, S. Kera, N. Ueno, Photoelectron spectroscopy on single crystals of organic semiconductors: experimental electronic band structure for optoelectronic properties, J. Mater. Chem. C 8 (2020) 9090–9132, https://doi.org/10.1039/D0TC00891E.
[2] S. Machida, Y. Nakayama, S. Duhm, Q. Xin, A. Funakoshi, N. Ogawa, S. Kera, N. Ueno, H. Ishii, Highest-occupied-molecular-orbital band dispersion of rubrene single crystals as observed by angle-resolved ultraviolet photoelectron spectroscopy, Phys. Rev. Lett. 104 (2010) 156401, https://doi.org/10.1103/PhysRevLett.104.156401.
[3] S. Sharifzadeh, P. Darancet, L. Kronik, J.B. Neaton, Low-energy charge-transfer excitons in organic solids from first-principles: the case of pentacene, J. Phys. Chem. Lett. 4 (2013) 2197–2201, https://doi.org/10.1021/jz401069f.
[4] A.M. Valencia, D. Bischof, S. Anhäuser, M. Zeplichal, A. Terfort, G. Witte, C. Cocchi, Excitons in organic materials: revisiting old concepts with new insights, Electron. Struct. 5 (2023) 033003, https://doi.org/10.1088/2516-1075/acf2d4.
[5] H. Ibach, D.L. Mills, Electron Energy Loss Spectroscopy and Surface Vibrations, Elsevier, 1982, https://doi.org/10.1016/C2013-0-10894-X.
[6] J. Fink, Recent developments in energy-loss spectroscopy, in: 1989: pp. 121–232. ⟨https://doi.org/10.1016/S0065-2539(08)60947-6⟩.
[7] R. Brydson, Electron Energy Loss Spectroscopy, Garland Science, 2020, https://doi.org/10.1201/9781003076858.
[8] A. Politano, On the fate of high-resolution electron energy loss spectroscopy (HREELS), a versatile probe to detect surface excitations: will the Phoenix rise again? Phys. Chem. Chem. Phys. 23 (2021) 26061–26069, https://doi.org/10.1039/D1CP03804D.
[9] M. Ichikawa, Inelastic scattering of low-energy electrons from a crystal surface, Phys. Rev. B. 10 (1974) 2416–2428, https://doi.org/10.1103/PhysRevB.10.2416.
[10] Y. Ohkawa, K. Yamada, T. Kawamura, Nature of angle-resolved electron energy loss spectrum, J. Phys. Soc. Jpn. 52 (1983) 338–343, https://doi.org/10.1143/JPSJ.52.338.
[11] H. Ibach, F.C. Bocquet, J. Sforzini, S. Soubatch, F.S. Tautz, Electron energy loss spectroscopy with parallel readout of energy and momentum, Rev. Sci. Instrum. 88 (2017) 033903, https://doi.org/10.1063/1.4977529.
[12] M. Knupfer, H. Berger, Dispersion of electron–hole excitations in pentacene along (100), Chem. Phys. 325 (2006) 92–98, https://doi.org/10.1016/j.chemphys.2005.06.044.
[13] R. Schuster, M. Knupfer, D.R.T. Zahn, H. Berger, Anisotropic dynamic response of pentacene single crystals, Eur. Phys. J. B. 59 (2007) 25–28, https://doi.org/10.1140/epjb/e2007-00256-6.
[14] F. Roth, R. Schuster, A. König, M. Knupfer, H. Berger, Momentum dependence of the excitons in pentacene, J. Chem. Phys. 136 (2012) 204708, https://doi.org/10.1063/1.4723812.
[15] F. Roth, B. Mahns, S. Hampel, M. Nohr, H. Berger, B. Büchner, M. Knupfer, Exciton properties of selected aromatic hydrocarbon systems, Eur. Phys. J. B 86 (2013) 66, https://doi.org/10.1140/epjb/e2012-30592-1.
[16] M.P. Seah, W.A. Dench, Quantitative electron spectroscopy of surfaces: a standard data base for electron inelastic mean free paths in solids, Surf. Interface Anal. 1 (1979) 2–11, https://doi.org/10.1002/sia.740010103.
[17] Y. Ozawa, Y. Nakayama, S. Machida, H. Kinjo, H. Ishii, Maximum probing depth of low-energy photoelectrons in an amorphous organic semiconductor film, J. Electron Spectrosc. Relat. Phenom. 197 (2014) 17–21, https://doi.org/10.1016/j.elspec.2014.08.001.
[18] F.S. Tautz, S. Sloboshanin, J.A. Schaefer, R. Scholz, V. Shklover, M. Sokolowski, E. Umbach, Vibrational properties of ultrathin PTCDA films on Ag(110), Phys. Rev. B. 61 (2000) 16933–16947, https://doi.org/10.1103/PhysRevB.61.16933.
[19] F.S. Tautz, M. Eremtchenko, J.A. Schaefer, M. Sokolowski, V. Shklover, E. Umbach, Strong electron-phonon coupling at a metal/organic interface: PTCDA/Ag(111), Phys. Rev. B. 65 (2002) 125405, https://doi.org/10.1103/PhysRevB.65.125405.
[20] K. Fujii, S. Kera, M. Oiwa, K.K. Okudaira, K. Sakamoto, N. Ueno, Influence of intramolecular vibrations in charge redistribution at the pentacene–graphite interface, Surf. Sci. 601 (2007) 3765–3768, https://doi.org/10.1016/j.susc.2007.04.027.
[21] K. Fujii, C. Himcinschi, M. Toader, S. Kera, D.R.T. Zahn, N. Ueno, Vibrational properties of perfluoropentacene thin film, J. Electron Spectrosc. Relat. Phenom. 174 (2009) 65–69, https://doi.org/10.1016/j.elspec.2009.01.002.
[22] P. Amsalem, L. Giovanelli, J.M. Themlin, T. Angot, Electronic and vibrational properties at the ZnPc/Ag(110) interface, Phys. Rev. B 79 (2009) 235426, https://doi.org/10.1103/PhysRevB.79.235426.
[23] P. Navarro, F.C. Bocquet, I. Deperasińska, G. Pirug, F.S. Tautz, M. Orrit, Electron energy loss of terrylene deposited on Au(111): vibrational and electronic spectroscopy, J. Phys. Chem. C 119 (2015) 277–283, https://doi.org/10.1021/jp5086262.
[24] I. Kröger, B. Stadtmüller, C. Kumpf, Submonolayer and multilayer growth of titaniumoxide-phthalocyanine on Ag(111), N. J. Phys. 18 (2016) 113022, https://doi.org/10.1088/1367-2630/18/11/113022.
[25] J. Sforzini, F.C. Bocquet, F.S. Tautz, Adsorption-induced symmetry reduction of metal-phthalocyanines studied by vibrational spectroscopy, Phys. Rev. B. 96 (2017) 165410, https://doi.org/10.1103/PhysRevB.96.165410.
[26] M.L. Tiago, J.E. Northrup, S.G. Louie, Ab initio calculation of the electronic and optical properties of solid pentacene, Phys. Rev. B 67 (2003) 115212, https://doi.org/10.1103/PhysRevB.67.115212.
[27] Y.C. Cheng, R.J. Silbey, D.A. da Silva Filho, J.P. Calbert, J. Cornil, J.L. Brédas, Three-dimensional band structure and bandlike mobility in oligoacene single crystals: a theoretical investigation, J. Chem. Phys. 118 (2003) 3764–3774, https://doi.org/10.1063/1.1539090.
[28] N. Koch, A. Vollmer, I. Salzmann, B. Nickel, H. Weiss, J.P. Rabe, Evidence for temperature-dependent electron band dispersion in pentacene, Phys. Rev. Lett. 96 (2006) 156803, https://doi.org/10.1103/PhysRevLett.96.156803.
[29] H. Kakuta, T. Hirahara, I. Matsuda, T. Nagao, S. Hasegawa, N. Ueno, K. Sakamoto, Electronic structures of the highest occupied molecular orbital bands of a pentacene ultrathin film, Phys. Rev. Lett. 98 (2007) 247601, https://doi.org/10.1103/PhysRevLett.98.247601.

[30] H. Yoshida, N. Sato, Crystallographic and electronic structures of three different polymorphs of pentacene, Phys. Rev. B 77 (2008) 235205, https://doi.org/10.1103/PhysRevB.77.235205.
[31] M. Ohtomo, T. Suzuki, T. Shimada, T. Hasegawa, Band dispersion of quasi-single crystal thin film phase pentacene monolayer studied by angle-resolved photoelectron spectroscopy, Appl. Phys. Lett. 95 (2009) 123308, https://doi.org/10.1063/1.3232205.
[32] R.C. Hatch, D.L. Huber, H. Höchst, Electron-phonon coupling in crystalline pentacene films, Phys. Rev. Lett. 104 (2010) 047601, https://doi.org/10.1103/PhysRevLett.104.047601.
[33] Y. Nakayama, Y. Mizuno, M. Hikasa, M. Yamamoto, M. Matsunami, S. Ideta, K. Tanaka, H. Ishii, N. Ueno, Single-crystal pentacene valence-band dispersion and its temperature dependence, J. Phys. Chem. Lett. 8 (2017) 1259–1264, https://doi.org/10.1021/acs.jpclett.7b00082.
[34] Y. Nakayama, M. Hikasa, N. Moriya, M. Meissner, T. Yamaguchi, K. Yoshida, M. Murata, K. Mase, T. Ueba, S. Kera, Anisotropic valence band dispersion of single crystal pentacene as measured by angle-resolved ultraviolet photoelectron spectroscopy, J. Mater. Res. 33 (2018) 3362–3370, https://doi.org/10.1557/jmr.2018.315.
[35] H. Sato, S.A. Abd. Rahman, Y. Yamada, H. Ishii, H. Yoshida, Conduction band structure of high-mobility organic semiconductors and partially dressed polaron formation, Nat. Mater. 21 (2022) 910–916, https://doi.org/10.1038/s41563-022-01308-z.
[36] Y.-Y. Lin, D.J. Gundlach, S.F. Nelson, T.N. Jackson, Stacked pentacene layer organic thin-film transistors with improved characteristics, IEEE Electron. Device Lett. 18 (1997) 606–608, https://doi.org/10.1109/55.644085.
[37] H. Klauk, M. Halik, U. Zschieschang, G. Schmid, W. Radlik, W. Weber, High-mobility polymer gate dielectric pentacene thin film transistors, J. Appl. Phys. 92 (2002) 5259–5263, https://doi.org/10.1063/1.1511826.
[38] O.D. Jurchescu, J. Baas, T.T.M. Palstra, Effect of impurities on the mobility of single crystal pentacene, Appl. Phys. Lett. 84 (2004) 3061–3063, https://doi.org/10.1063/1.1704874.
[39] M.B. Smith, J. Michl, Singlet fission, Chem. Rev. 110 (2010) 6891–6936, https://doi.org/10.1021/cr1002613.
[40] C. Jundt, G. Klein, B. Sipp, J. Le Moigne, M. Joucla, A.A. Villaeys, Exciton dynamics in pentacene thin films studied by pump-probe spectroscopy, Chem. Phys. Lett. 241 (1995) 84–88, https://doi.org/10.1016/0009-2614(95)00603-2.
[41] P.M. Zimmerman, F. Bell, D. Casanova, M. Head-Gordon, Mechanism for singlet fission in pentacene and tetracene: from single exciton to two triplets, J. Am. Chem. Soc. 133 (2011) 19944–19952, https://doi.org/10.1021/ja208431r.
[42] D. Beljonne, H. Yamagata, J.L. Brédas, F.C. Spano, Y. Olivier, Charge-transfer excitations steer the davydov splitting and mediate singlet exciton fission in pentacene, Phys. Rev. Lett. 110 (2013) 226402, https://doi.org/10.1103/PhysRevLett.110.226402.
[43] J. Zirzlmeier, D. Lehnherr, P.B. Coto, E.T. Chernick, R. Casillas, B.S. Basel, M. Thoss, R.R. Tykwinski, D.M. Guldi, Singlet fission in pentacene dimers, Proc. Natl. Acad. Sci. USA 112 (2015) 5325–5330, https://doi.org/10.1073/pnas.1422436112.
[44] Y. Nakayama, R. Tsuruta, T. Koganezawa, 'Molecular beam epitaxy' on organic semiconductor single crystals: characterization of well-defined molecular interfaces by synchrotron radiation X-ray diffraction techniques, Materials 15 (2022) 7119, https://doi.org/10.3390/ma15207119.
[45] Y. Nakayama, Y. Mizuno, T. Hosokai, T. Koganezawa, R. Tsuruta, A. Hinderhofer, A. Gerlach, K. Broch, V. Belova, H. Frank, M. Yamamoto, J. Niederhausen, H. Glowatzki, J.P. Rabe, N. Koch, H. Ishii, F. Schreiber, N. Ueno, Epitaxial growth of an organic p–n heterojunction: C 60 on single-crystal pentacene, ACS Appl. Mater. Interfaces 8 (2016) 13499–13505, https://doi.org/10.1021/acsami.6b02744.
[46] Y. Mizuno, M. Yamamoto, H. Kinjo, K. Mase, H. Ishii, K.K. Okudaira, H. Yoshida, Y. Nakayama, Effects of the ambient exposure on the electronic states of the clean surface of the pentacene single crystal, Mol. Cryst. Liq. Cryst. 648 (2017) 216–222, https://doi.org/10.1080/15421406.2017.1302001.
[47] Y. Nakayama, Y. Uragami, M. Yamamoto, K. Yonezawa, K. Mase, S. Kera, H. Ishii, N. Ueno, High-resolution core-level photoemission measurements on the pentacene single crystal surface assisted by photoconduction, J. Phys. Condens. Matter 28 (2016) 094001, https://doi.org/10.1088/0953-8984/28/9/094001.
[48] Y. Nakayama, J. Miyamoto, K. Yamauchi, Y. Baba, F. Teshima, K. Tanaka, Far- and mid-infrared FT-IR analysis of the single-crystal pentacene using a linearly polarized synchrotron radiation light source, Vib. Spectrosc. 132 (2024) 103681, https://doi.org/10.1016/j.vibspec.2024.103681.
[49] D. Faltermeier, B. Gompf, M. Dressel, A.K. Tripathi, J. Pflaum, Optical properties of pentacene thin films and single crystals, Phys. Rev. B 74 (2006) 125416, https://doi.org/10.1103/PhysRevB.74.125416.
[50] D. Qi, H. Su, M. Bastjan, O.D. Jurchescu, T.M. Palstra, A.T.S. Wee, M. Rübhausen, A. Rusydi, Observation of Frenkel and charge transfer excitons in pentacene single crystals using spectroscopic generalized ellipsometry, Appl. Phys. Lett. 103 (2013), https://doi.org/10.1063/1.4811758.
[51] P. Cudazzo, M. Gatti, A. Rubio, F. Sottile, Frenkel versus charge-transfer exciton dispersion in molecular crystals, Phys. Rev. B 88 (2013) 195152, https://doi.org/10.1103/PhysRevB.88.195152.
[52] N.J. Hestand, H. Yamagata, B. Xu, D. Sun, Y. Zhong, A.R. Harutyunyan, G. Chen, H.-L. Dai, Y. Rao, F.C. Spano, Polarized absorption in crystalline pentacene: theory vs experiment, J. Phys. Chem. C. 119 (2015) 22137–22147, https://doi.org/10.1021/acs.jpcc.5b07163.
[53] M. Grobosch, R. Schuster, T. Pichler, M. Knupfer, H. Berger, Analysis of the anisotropy of excitons in pentacene single crystals using reflectivity measurements and electron energy-loss spectroscopy, Phys. Rev. B 74 (2006) 155202, https://doi.org/10.1103/PhysRevB.74.155202.
[54] R. Schuster, M. Knupfer, H. Berger, Exciton band structure of pentacene molecular solids: breakdown of the frenkel exciton model, Phys. Rev. Lett. 98 (2007) 037402, https://doi.org/10.1103/PhysRevLett.98.037402.
[55] C.C. Mattheus, A.B. Dros, J. Baas, A. Meetsma, J.L. de Boer, T.T.M. Palstra, Polymorphism in pentacene, Acta Crystallogr. Sect. C. Cryst. Struct. Commun. 57 (2001) 939–941, https://doi.org/10.1107/S010827010100703X.
[56] T. Fujita, M.K. Alam, T. Hoshi, Thousand-atom ab initio calculations of excited states at organic/organic interfaces: toward first-principles investigations of charge photogeneration, Phys. Chem. Chem. Phys. 20 (2018) 26443–26452, https://doi.org/10.1039/C8CP05574B.
[57] M. Iwasawa, R. Tsuruta, Y. Nakayama, M. Sasaki, T. Hosokai, S. Lee, K. Fukumoto, Y. Yamada, Exciton dissociation and electron transfer at a well-defined organic interface of an epitaxial C 60 layer on a pentacene single crystal, J. Phys. Chem. C 124 (2020) 13572–13579, https://doi.org/10.1021/acs.jpcc.0c02796.
[58] Y. Nakayama, F.C. Bocquet, R. Tsuruta, S. Soubatch, F.S. Tautz, Replication Data for: Anisotropic dispersion of excitonic bands of the single-crystal pentacene (001) surface as measured by low-energy angle-resolved high-resolution electron energy-loss spectroscopy, Jülich DATA (2025), https://doi.org/10.26165/JUELICH-DATA/WUFYPE.